AJNR

Neuroimaging of acoustic nerve sheath tumors after stereotaxic radiosurgery.

M E Linskey, L D Lunsford and J C Flickinger

AJNR Am J Neuroradiol 1991, 12 (6) 1165-1175
http://www.ajnr.org/content/12/6/1165

Neuroimaging of Acoustic Nerve Sheath Tumors After Stereotaxic Radiosurgery

Mark E. Linskey[1]
L. Dade Lunsford[1–3]
John C. Flickinger[3]

Using a strict method for measuring tumor size, we evaluated tumor response to radiosurgery in 88 patients with 89 acoustic tumors treated over 3 years with a 201-source cobalt-60 gamma unit. Overall, tumor size was unchanged in 73% of patients and increased in 4%. In 22% of patients, tumor diameter decreased an average of 4.9 mm 3–33 months after treatment. Tumor shrinkage occurred in 36% of 50 patients who were followed for at least 1 year after treatment. Loss of tumor contrast enhancement was seen in 79% of patients 1–18 months after treatment. Delayed communicating hydrocephalus developed in four patients. In eight patients, increased signal on T2-weighted MR images developed in the adjacent cerebellar peduncle (n = 5) or the peduncle and dorsolateral pons (n = 3) 5–15 months after treatment. T1-weighted MR imaging and CT were insensitive to these adjacent brain changes.

Stereotaxic radiosurgery is an important alternative treatment for selected patients with acoustic tumors. There is no mortality or major perioperative morbidity, hospitalization time and costs are smaller than for microsurgery, patient employment or functional level is maintained, and hearing preservation and facial neuropathy rates are comparable to those in published microsurgical series. Although the rate of occurrence of trigeminal neuropathy is greater than those reported in published microsurgical series, the majority of cases are mild, transient, and nondebilitating. MR imaging before and after radiosurgery is the most sensitive imaging tool to evaluate tumor response, the presence of adjacent parenchymal signal changes, and ventricular size. With a mean follow-up time of 14.6 months, the rate of complications detected by neuroimaging is low and the tumor control rate is 96%.

AJNR **12:1165–1175, November/December 1991**

Stereotaxic radiosurgery refers to precise, mechanically directed, closed-skull destruction of an intracranial target by ionizing beams of radiation delivered during a single treatment session [1]. This treatment has been performed by using the multisource cobalt-60 gamma unit [1–7] and, more recently, with modified linear accelerators [8–11]. In 1969, Lars Leksell [12] was the first to use the gamma unit for the treatment of an acoustic tumor. Since then, more than 500 patients with acoustic tumors have undergone stereotaxic radiosurgery worldwide [3–5, 13, 14].

Previously published reports have documented hearing preservation rates and frequency of cranial neuropathy after radiosurgery comparable to those achieved with microsurgery [4, 5, 13, 14]. While reports of tumor control rates after radiosurgery appear promising, no report has documented the measurement criteria used to determine whether a tumor enlarged or shrank, or objectively documented the magnitude of the size change. In this study we describe our method for measuring changes in tumor size and systematically examine the postoperative neuroimaging findings in 88 patients with a total of 89 acoustic tumors treated by means of a 201-source cobalt-60 gamma unit over a 3-year period. In addition, we define the rate of treatment complications detectable with neuroimaging. The clinical results after treatment in the same group of patients have been reported in detail

Received February 15, 1991, revision requested April 17, 1991; revision received May 24, 1991; accepted May 28, 1991.

[1] Department of Neurological Surgery, University of Pittsburgh School of Medicine and the Specialized Neurosurgical Center of Presbyterian University Hospital, 230 Lothrop St., Pittsburgh, PA 15213, Address reprint requests to L. Dade Lunsford.

[2] Department of Radiology, University of Pittsburgh School of Medicine and the Specialized Neurosurgical Center of Presbyterian University Hospital, Pittsburgh, PA 15213.

[3] Department of Radiation Oncology, University of Pittsburgh School of Medicine and the Specialized Neurosurgical Center of Presbyterian University Hospital, Pittsburgh, PA 15213.

0195–6108/91/1206–1165

elsewhere (Linskey ME et al., *Neurosurgery Clinics of North America*, in press).

Subjects and Methods

Patient Population

At our institution, 101 patients with a total of 102 acoustic tumors were treated by stereotaxic radiosurgery over a 3-year period. Patients were selected for radiosurgery if they fulfilled one or more of the following criteria: (1) the patient was elderly, (2) the patient had significant medical problems posing an excessive surgical risk, (3) the tumor was present in the patient's only hearing ear, (4) the patient had bilateral acoustic tumors, (5) direct surgical removal was refused by a patient who requested radiosurgery instead, (6) prior surgery had failed to control tumor growth.

The patients' ages ranged from 14 to 83 years (median, 60 years). Most younger patients had neurofibromatosis, type II (15 patients). In one patient, bilateral tumors were treated separately, 1 year apart. A pathologic diagnosis of acoustic nerve sheath tumor was confirmed prior to radiosurgery in 20 patients who had undergone a previous microsurgical resection (23%) and after radiosurgery in two patients who subsequently underwent microsurgical resection (2%). In the remaining 66 patients (67 tumors), the radiologic diagnosis of acoustic nerve sheath tumor was based on the presence of an enhancing extraaxial mass in the cerebellopontine angle centered at, and entering into, the porus acousticus with enlargement of the internal auditory canal [15, 16]. A minimum of 3 months of clinical follow-up data were available in 92 of 101 patients. Neuroimaging follow-up results were available in 88 of these patients (97%) with a total of 89 tumors. The mean time of neuroimaging follow-up was 14.6 months (SD, 8.8 months). The neuroimaging results of these 88 patients form the subject of this report.

TABLE 1: Dose Plans

Characteristic	Number (%) of Tumors (n = 89)
Tumor-margin dose (Gy):	
12–15.99	6 (7)
16–16.99	16 (18)
17–17.99	15 (17)
18–19.99	18 (20)
20	34 (38)
Maximum tumor dose (Gy):	
24.3–31.99	15 (17)
32–33.99	23 (26)
34–35.99	11 (12)
36–39.99	17 (19)
40	20 (22)
40.01–50	3 (3)
Tumor-margin isodose (%):	
40	6 (7)
45	1 (1)
50	59 (66)
55	5 (6)
60	10 (11)
70	8 (9)

Treatment Technique

Detailed descriptions of dose planning [17–19] and the treatment technique [13, 14] using the 201-source cobalt-60 gamma unit have been published previously. Eighty-two tumors (92%) were treated at an isodose of 50% or greater at the tumor margin. Of those 82, 79 received a margin dose of ≥16 Gy, 64 received ≥17 Gy, and 49 received ≥18 Gy. Because of suboptimal size, markedly irregular three-dimensional tumor volumes, the need to provide complete tumor coverage, or the need to spare critical brain structures, six patients had to be treated at the 40% isodose and one patient at the 45% isodose at the tumor margin. The maximum tumor doses and the tumor-margin doses and isodoses are presented in Table 1. Multiple irradiation isocenters were used frequently (average, 2.4 per patient; range, 1–8). A multiplanar example of a multi-isocenter dose plan is presented in Figure 1.

Neuroimaging

High-resolution (General Electric 9800 scanner, General Electric Medical Systems Division, Milwaukee, WI) contrast-enhanced CT scanning, with 5-mm-thick axial slices and 3-mm table incrementation, was performed at the time of target localization, prior to irradiation. Sagittal and coronal reformatted images supplemented the imaging data base in each case. This scan provided the baseline images for subsequent comparisons. Most patients also had preoperative MR imaging. Patients underwent serial follow-up contrast-enhanced CT or MR imaging at 3-month intervals during the first year, 6-month intervals for the second year, and on a yearly basis thereafter.

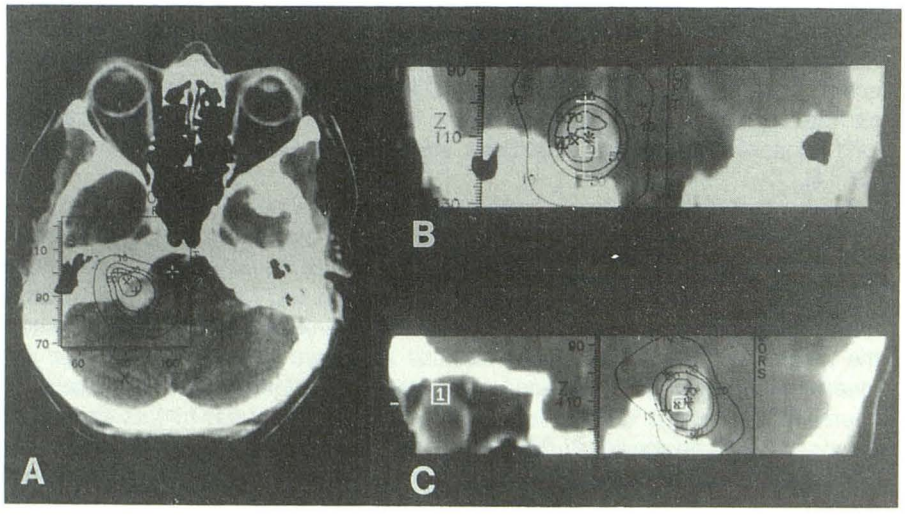

Fig. 1.—*A–C*, Dose-planning contrast-enhanced axial CT (*A*) with coronal (*B*) and sagittal (*C*) reconstructions show isodose curves in all three planes. This tumor in a 73-year-old woman was treated with two isocenters delivering 20 Gy to the tumor margin at the 50% isodose line.

Neuroimaging follow-up consisted solely of MR in 60 patients, MR and CT in 16 patients, and CT alone in 12 patients (13 tumors). All but two follow-up CT scans were contrast enhanced. All follow-up MR studies consisted of T1- and T2-weighted, unenhanced images. T1-weighted contrast-enhanced images were obtained in 73 of 76 cases with follow-up MR imaging. At our institution the T1-weighted enhanced image is taken immediately after the completion of the IV gadopentetate dimeglumine infusion. Because some patients lived long distances from our institution, some imaging studies were obtained by referring physicians and reviewed at our institution.

Measurements

To arrive at objective tumor size, we made five measurements (X, Y, A, B, and C) of each tumor, as outlined in Figure 2. Measurements were made directly from film, using fine calipers. All measurements were made by the same person using the same technique. Caliper measurements had a precision of ±3% (mean SD of 10 measurements, each repeated 10 times). Measurement X represents the cross-sectional diameter of midpoint of the bony edges of the internal auditory canal. Measurement Y is the length of the internal auditory canal from the fundus to a line drawn along the face of the petrous bone at the canal exit. The maximum tumor diameter was measured three ways: perpendicular to the surface of the petrous bone (A), parallel to the surface of the petrous bone (B), and vertically in the reformatted coronal plane (C). Measurements A and B were not always taken from the same axial image.

The average tumor diameter was defined as $D = (A + B + C)/3$. The technical measurement error for both A and B was estimated to be ±0.5 mm; for C, it was ±3 mm (equivalent to one table increment), which led to a calculated measurement error for D of ±1.3 mm. For purposes of this study, we considered the average tumor diameter after treatment to be "objectively different" from the pretreatment size if it changed at least ±2.6 mm (twice the calculated measurement error for D). The distribution of preoperative tumor size and volume is presented in Table 2. Average tumor diameter ranged from intracanalicular to 32.7 mm (median, 17.8 mm).

Tumor volumes were calculated from X, Y, and D. Total tumor volume was considered to be equal to the *intracanalicular* tumor volume $[(\pi)(X)(X)(Y)/6]$ plus the *cerebellopontine angle (CPA)* tumor volume $[4\pi(D/2)^3/3]$. The change in *CPA* tumor volume necessary to consider the two volumes "objectively different" was a function of measurement error and varied according to the magnitude of D, as shown by the dashed curves in Figure 3.

Results

Tumor Size

The scattergram in Figure 4 demonstrates the measured change in average tumor diameter from the time of treatment to follow-up for each patient. Comparing these two measured tumor diameters and using the strict definition of measurement error as described, we found that postradiosurgical tumor size was reduced in 22% of patients, unchanged in 73%, and increased in 4%. Objectively defined tumor shrinkage was seen between 3 and 33 months (median, 12 months) after treatment, and the rate of tumor shrinkage increased with longer follow-up, as shown in Table 3. In patients with a minimum of 1 year of neuroimaging follow-up, tumor size decreased in 36%, remained unchanged in 58%, and increased in 6%. In the 20 patients with tumor shrinkage, the

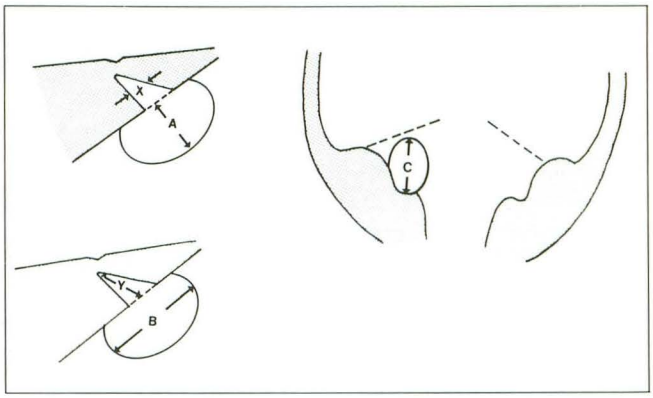

Fig. 2.—Schematic shows the five measurements taken of each acoustic tumor (see text for a description of each measurement).

TABLE 2: Preoperative Tumor Size

Characteristic	Number (%) of Tumors (n = 89)
Average tumor diameter[a] (cm):	
Intracanalicular	3 (3)
<1	9 (10)
1–1.99	49 (55)
2–2.99	25 (28)
≥3	3 (3)
Tumor volume (cm^3):	
<1	15 (17)
1–2.99	24 (27)
3–5.99	31 (35)
6–10	8 (9)
>10	11 (12)

[a] Tumor diameter refers to the portion of the tumor within the cerebellopontine angle. The intracanalicular portion of the tumor is considered separately.

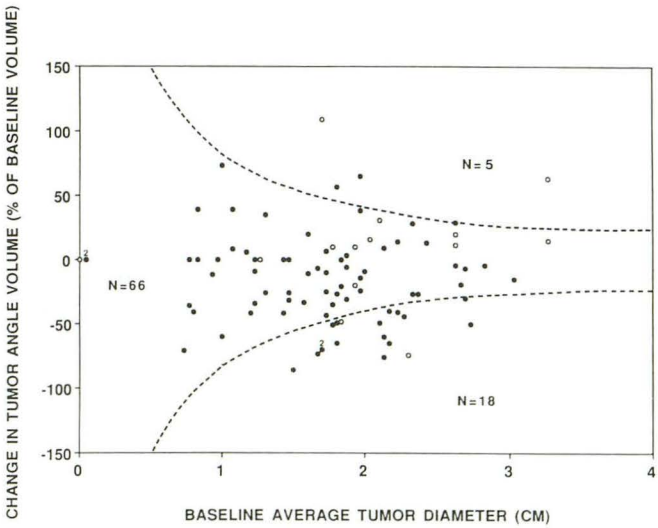

Fig. 3.—Graph shows calculated change in cerebellopontine angle volume (see text) from pretreatment to follow-up for each tumor vs baseline average tumor diameter. *Dashed curves* depict the difference necessary to consider pre- and posttreatment values "objectively different," given the inherent measurement error.

average decrease in tumor diameter was 4.9 mm (SD, 1.6 mm).

Comparing the calculated change in *CPA* tumor volume after radiosurgery against baseline *CPA* tumor volume, we found that tumor size was reduced in 20% of patients, unchanged in 74%, and larger in 6% (Fig. 3). In the 18 patients with decreased *CPA* tumor volumes, the mean volume decrease was 57% (SD, 15%).

Two patients who had delayed tumor growth also exhibited increased mass effect on neuroimaging. Both patients had neurofibromatosis, type II. Only one patient required surgical decompression because of increased mass effect. Changes in tumor size were not significantly associated with initial tumor size, tumor-margin dose, maximal tumor dose, tumor margin isodose, or the presence of neurofibromatosis ($p < .15$, $p < .20$, $p < .20$, $p < .85$, $p < .60$, respectively; chi-square test).

Tumor Enhancement

Follow-up neuroimaging included contrast-enhanced CT or MR in 83 patients (94%). The other five patients were either allergic to iodine or unable to tolerate MR. Loss of central tumor enhancement was evident in 66 patients (79%) between 1 and 18 months after treatment (median, 6 months) (Figs. 5–7). Seventeen percent of patients who initially lost intratumoral contrast enhancement subsequently regained enhancement 6–29 months after loss (median, 13 months) (Fig. 6). Although loss of contrast enhancement appears to be a good prognostic sign for objective tumor shrinkage (18/20 tumors), this association is not yet statistically significant ($p < .50$, chi-square test).

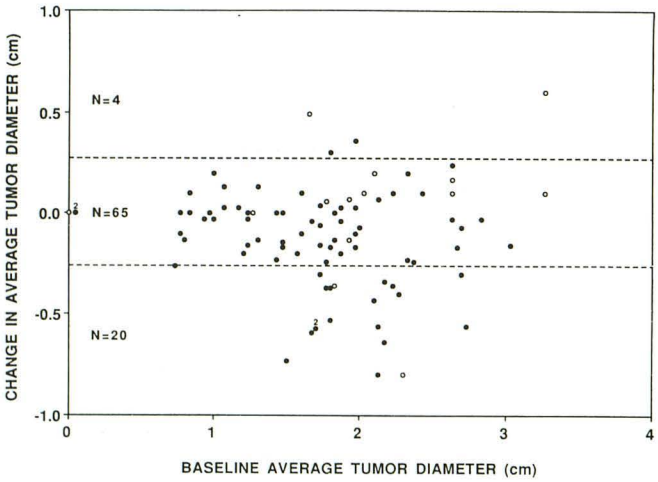

Fig. 4.—Graph shows change in average tumor diameter between treatment and follow-up for each tumor vs tumor diameter. *Dashed lines* depict the difference necessary to consider these two values "objectively different," given the inherent measurement error.

TABLE 3: Postoperative Tumor Size

Change	Overall No. (%)	≥12 Months Follow-up No. (%)	≥18 Months Follow-up No. (%)	≥24 Months Follow-up No. (%)
Increased	4 (4)	3 (6)	1 (3)	0
Unchanged	65 (73)	29 (58)	15 (52)	11 (58)
Decreased	20 (22)	18 (36)	13 (45)	8 (42)
Total	89	50	29	19

Hydrocephalus

Hydrocephalus developed in four patients (Fig. 8) 5–16 months after radiosurgery (median, 7.5 months). In none of these patients had the tumor increased in size. Two of the four had MR studies demonstrating periventricular increased signal on T2-weighted images consistent with transependymal absorption of CSF. The other two were followed solely with CT scans. None of the four had evidence of cerebral tissue loss that could account for their ventriculomegaly on an ex vacuo basis. All four underwent placement of a ventriculoperitoneal shunt. The CSF protein concentrations in three of the patients were 66, 57, and 46 mg/dl, respectively, at the time of shunting. The fourth patient's shunt was inserted at another institution, and her CSF protein concentration is not known.

Adjacent Parenchymal Changes

In eight patients (9%), follow-up neuroimaging demonstrated new findings characterized by increased signal intensity on T2-weighted MR images in the adjacent cerebellar peduncle alone ($n = 5$) or cerebellar peduncle and pons ($n = 3$) (Figs. 9 and 10). Onset of new parenchymal changes ranged from 5 to 15 months (median, 8 months). In all eight patients, the parenchymal changes were best detected by T2-weighted MR imaging. Intermediate-weighted scans were available in four patients and showed signal changes similar to those on T2-weighted scans. Imaging changes on contrast-enhanced T1-weighted studies, suggestive of blood-brain barrier breakdown, were observed in seven of the eight patients (Figs. 8 and 11). In each instance, a thin rim of contrast enhancement was visible 1–5 mm within the cerebellar peduncle, forming an arc parallel to the tumor margin. The enhanced T1-weighted image underestimated the volume of tissue affected, which was most clearly demonstrated on T2-weighted scans in each case.

In contrast to MR images, CT scans frequently failed to show parenchymal changes adjacent to the tumor. Hypodense regions in the cerebellar peduncle on CT were evident in only two of the eight patients, and in only one of these two patients was there a thin rim of iodinated contrast enhancement on CT (Fig. 12).

Follow-up MR images taken after the onset of parenchymal changes were available in six patients. Parenchymal T2 signal changes reverted to normal in two patients (one shown in Fig. 10) 14 and 19 months, respectively, after onset, but they had not yet resolved 4, 5, 7, and 12 months after onset in the remaining four. Neither pyramidal tract signs nor central facial paresis developed in the three patients who had MR signal changes in the pons. The presence of increased T2 signal in the cerebellar peduncle did not correlate significantly with

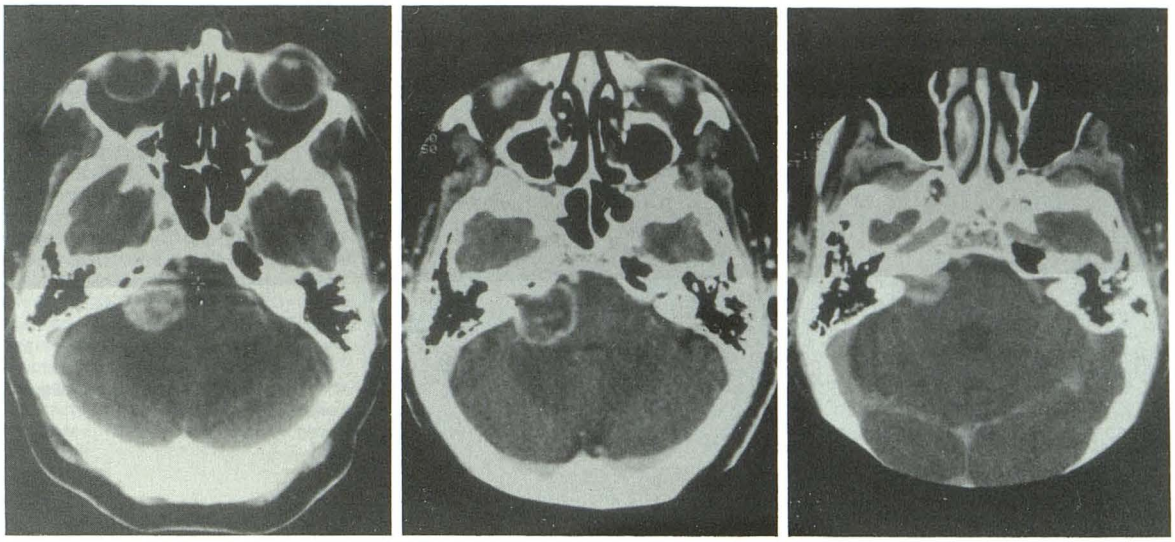

Fig. 5.—Contrast-enhanced CT scans of 63-year-old man whose right acoustic tumor was treated with stereotaxic radiosurgery (20 Gy at margin, 50% isodose).

A–C, Preoperative image (*A*); 3 months after treatment, decreased contrast enhancement was seen (*B*); 18 months after treatment, decreased tumor size was evident (*C*).

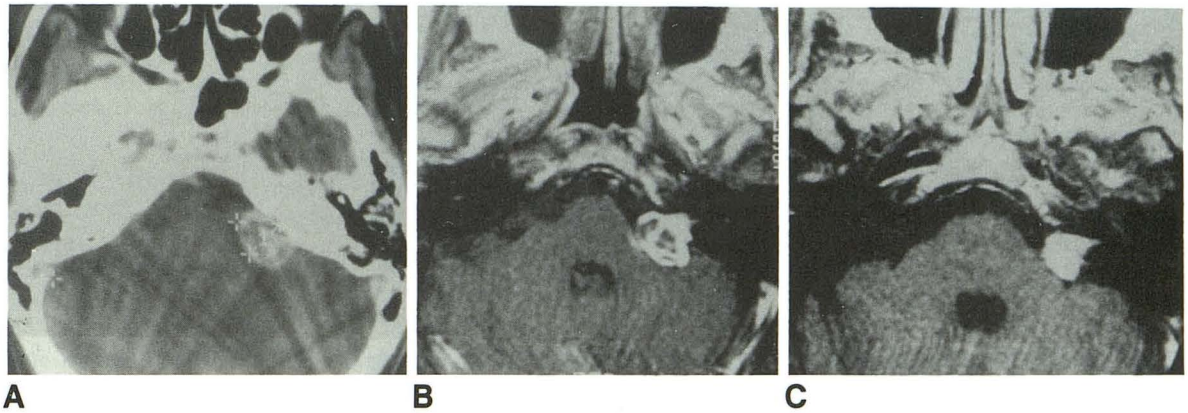

Fig. 6.—Contrast-enhanced neuroimaging of 68-year-old woman whose left acoustic tumor was treated with stereotaxic radiosurgery (20 Gy at margin, 50% isodose).

A–C, Preoperative CT scan (*A*); 12-month postoperative MR image (400/20/4) shows loss of central contrast enhancement (*B*); 32-month postoperative MR image (600/25) shows resumption of contrast enhancement and decrease in tumor size (*C*).

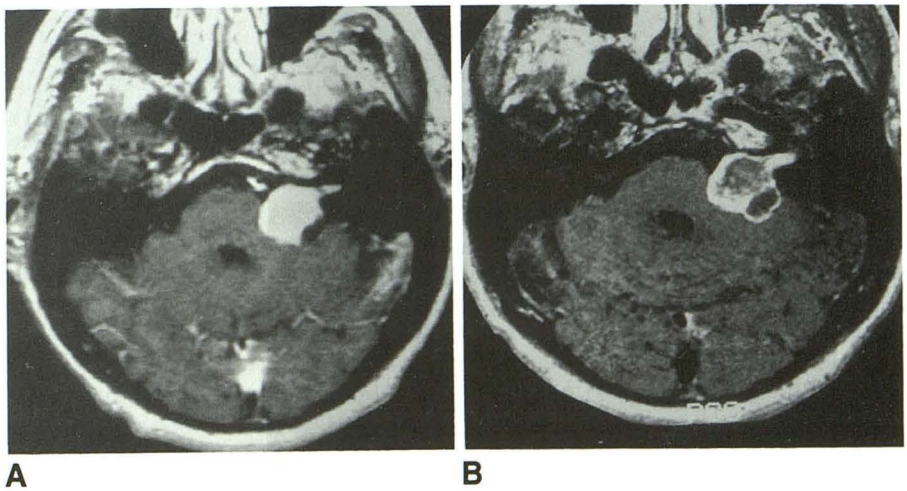

Fig. 7.—Contrast-enhanced MR images of 74-year-old man whose left acoustic tumor was treated with stereotaxic radiosurgery (16 Gy at margin, 50% isodose).

A and *B*, Preoperative MR image (600/30/4) (*A*); 6-month postoperative MR image (650/25) (*B*) shows marked loss of contrast enhancement.

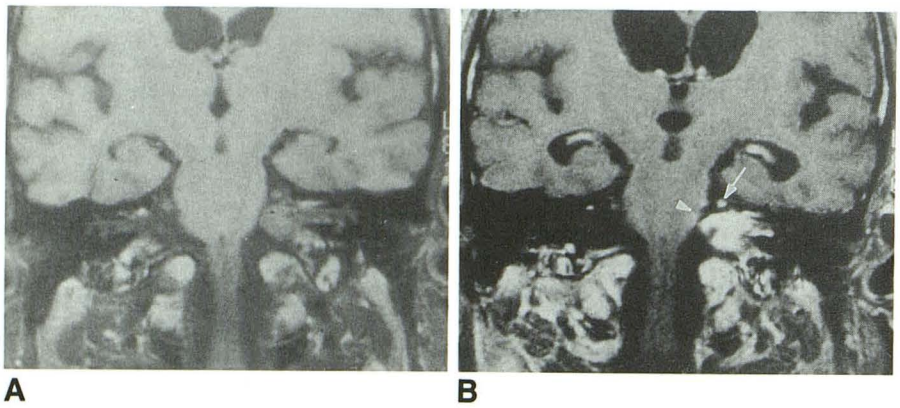

Fig. 8.—Coronal MR images of 64-year-old man in whom communicating hydrocephalus developed 15 months after stereotaxic radiosurgery (20 Gy at margin, 50% isodose) for a left acoustic tumor.

A and *B*, Preoperative image (700/20/4) (*A*); 15-month postoperative contrast-enhanced image (700/20) (*B*) shows ventriculomegaly without a change in tumor size, enhancement of ipsilateral trigeminal nerve (*arrow*), and a thin rim of enhancement in adjacent pons (*arrowhead*). Trigeminal nerve enhancement and brainstem enhancement resolved by the 20-month postoperative image but some increased signal in the peripheral pons on T2-weighted images persisted (*not shown*).

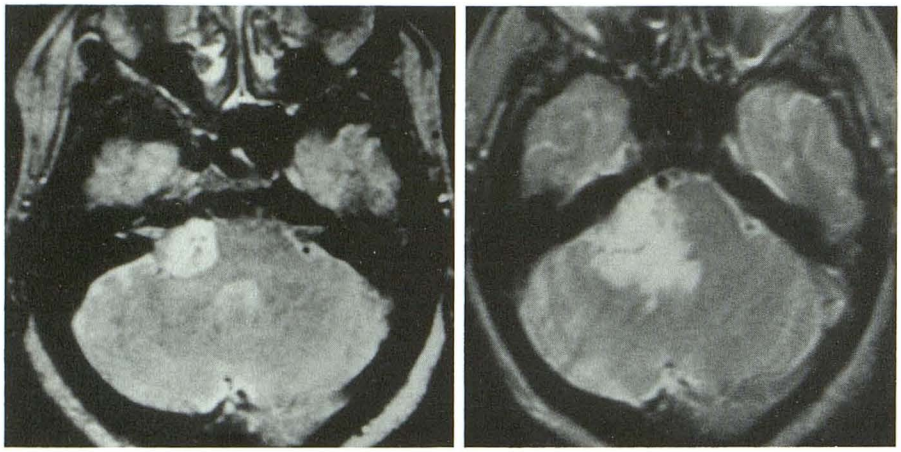

Fig. 9.—*A* and *B*, Axial MR images of 63-year-old man before stereotaxic radiosurgery (20 Gy at margin, 50% isodose) for a right acoustic tumor (2000/90/2) (*A*) and 6 months after treatment (2067/80) (*B*) show that increased signal developed in right cerebral peduncle and dorsolateral pons.

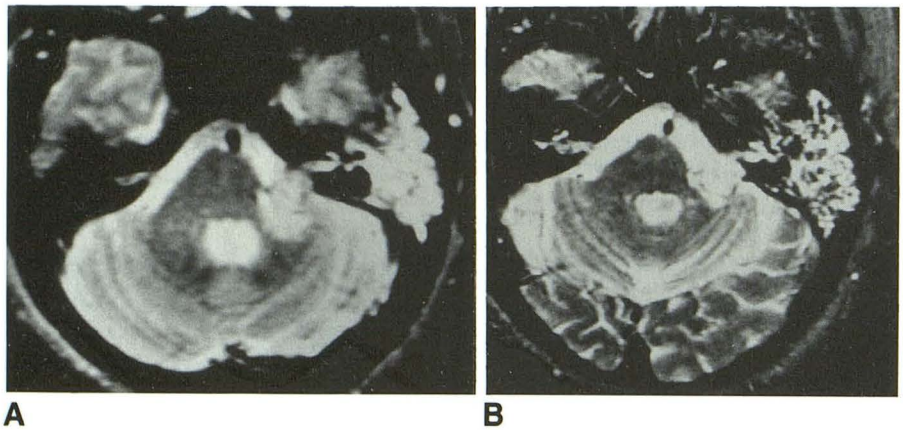

Fig. 10.—Axial MR images of 59-year-old woman whose left acoustic tumor was treated with stereotaxic radiosurgery (20 Gy at margin, 60% isodose).

A and *B*, 14 months after treatment (2867/80/2) increased signal was seen in left cerebellar peduncle (*A*); at 28 months (3429/90), these signal changes had resolved (*B*).

patient-reported delayed worsening of balance ($p < .50$, chi-square test). The postradiosurgery development of new adjacent parenchymal changes in the pons or cerebellar peduncle did not correlate significantly with tumor size, tumor-margin dose, maximum tumor dose, or tumor-margin isodose ($p < .80$, $p < .95$, $p < .95$, $p < .95$, respectively; chi-square test).

Clinical Sequelae

Ninety-one percent of patients were discharged from the hospital within 24 hr of treatment and 99% within 48 hr. All patients returned to their postoperative level of function or employment within 5–7 days of treatment. Functional level was maintained over a mean clinical follow-up of 20.5 months (range, 3–36 months).

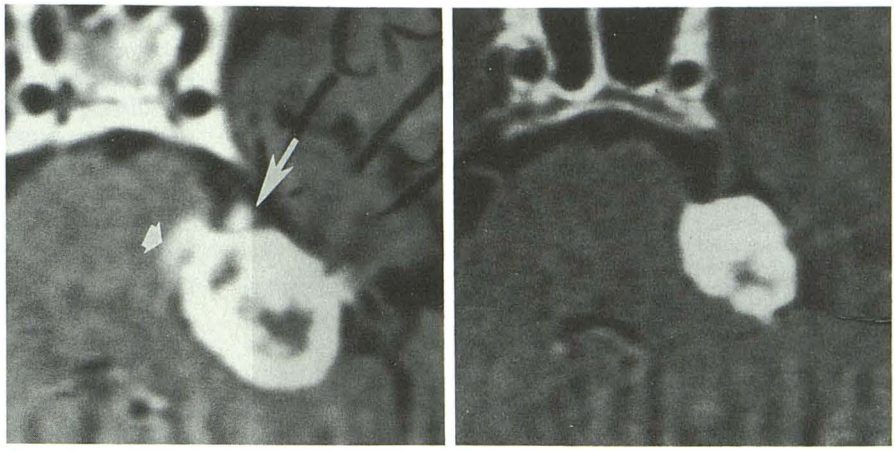

Fig. 11.—Contrast-enhanced MR images of 56-year-old woman who developed a previously undetected trigeminal neuropathy 7 months after treatment with stereotaxic radiosurgery (16 Gy at margin, 50% isodose).

***A*, Close-up image 9 months after radiosurgery (600/20/4) shows loss of intratumoral contrast enhancement, enhancement of trigeminal nerve root (*arrow*), and a small region of enhancement in adjacent pons (*arrowhead*).**

***B*, Close-up image 11 months later (20 months after radiosurgery) (500/20) shows resolution of both the trigeminal nerve enhancement and the brainstem enhancement. While the trigeminal neuropathy had significantly improved by the time of this image, some residual sensory paresthesia persisted. The brainstem enhancement was asymptomatic.**

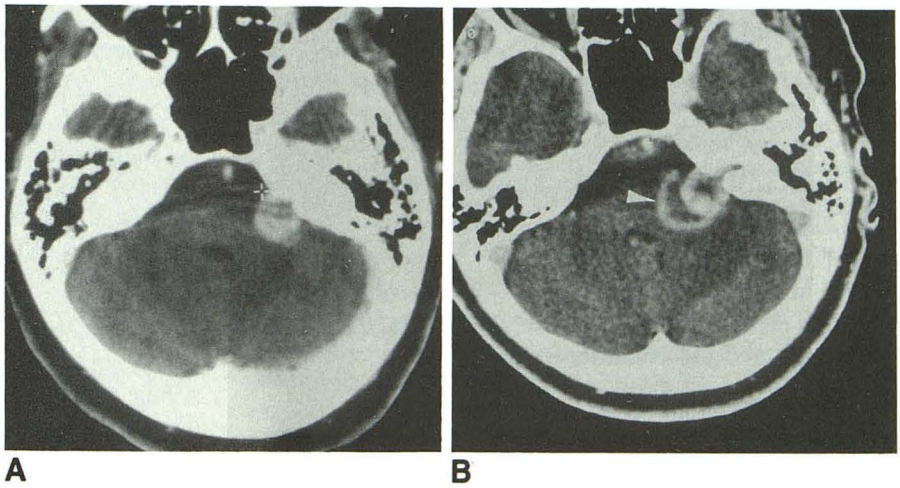

Fig. 12.—Axial contrast-enhanced CT scans of 59-year-old woman whose left acoustic tumor was treated with stereotaxic radiosurgery (20 Gy at margin, 60% isodose).

***A* and *B*, Before treatment (*A*) and 9 months after treatment (*B*), when a region of hypodensity was evident in the adjacent cerebellar peduncle, along with a thin surrounding rim of contrast enhancement, suggesting breakdown of the blood-brain barrier (*arrowhead*).**

Useful hearing, defined as Gardner and Robertson class I or II [20], was present in 19 patients preoperatively. Useful hearing preservation rates after radiosurgery were 50% at 6 months and 38% at 1 year. Median onset of useful hearing loss was 6 months after treatment (range, 1 week–1 year). Development of other delayed cranial neuropathies (ranging from mild to severe) included the onset of new facial neuropathy in 34%, trigeminal neuropathy in 32%, and glossopharyngeal neuropathy in one patient. The median onset of these cranial neuropathies was 5–6 months after treatment (range, 1–19 months).

Our strict follow-up criteria counted *any* subjective trigeminal numbness or paresthesia reported by a patient as an occurrence of trigeminal neuropathy *whether or not* decreased sensation could be demonstrated on neurologic examination. The vast majority of cases were mild, partial, and transient. No patient developed deafferentation pain or trigeminal motor neuropathy.

Facial-nerve function was graded according to the House-Brackmann grading system [21], and the pre- and postoperative scores for 91 patients with a minimum of 3 months follow-up are given in Table 4. Most new facial neuropathies were partial at onset and improved over time. Normal facial function eventually returned in 20% of patients who developed a delayed facial neuropathy, and 53% improved at least one grade. No patient whose sole treatment was radiosurgery was left with worse than grade IV facial function (two patients who underwent microsurgery at other institutions at the onset of facial neuropathy have permanent grade VI facial palsies). The overall rate of poor facial function (residual facial neuropathy greater than grade III) was 8%.

Twenty-nine percent of patients with no balance problems prior to surgery reported having worsened balance at some time after radiosurgery. In contrast, patients with abnormal balance were more likely to improve than worsen after radiosurgery (22% vs 14%). An overview of the postoperative clinical response after radiosurgery is presented in Table 5.

The rate of occurrence of trigeminal neuropathy correlated significantly with tumor size greater than 1 cm in average diameter ($p < .05$, Mantel-Haenzel log rank test) and with loss of tumor contrast enhancement ($p < .05$, chi-square with 1 degree of freedom). No cranial neuropathies or other complications correlated significantly with the presence or absence of neurofibromatosis or with a history of previous surgery at this tumor margin dose, the maximum tumor dose, or the tumor margin isodose. Our current number of patients

TABLE 4: Pre- and Postoperative Facial Nerve Function in 92 Tumors in 91 Patients[a]

Grade	Description	Number (%) of Tumors	
		Preoperative	Postoperative
I	Normal	70 (76)	52 (57)
II	Mild dysfunction	8 (9)	11 (12)
III	Moderate dysfunction	4 (4)	12 (13)
IV	Moderately severe dysfunction	2 (2)	8 (9)
V	Severe dysfunction	2 (2)	2 (2)
VI	Total paralysis	6 (7)	7 (8)

[a] House-Brackmann facial nerve grading system [21].

TABLE 5: Postoperative Clinical Response[a]

	% of Patients
1. Hospital discharge within 48 hr	99
2. Return to previous employment or functional level within 5–7 days	100
3. Functional level maintained over the period of follow-up	100
4. One year useful hearing preservation rate	38
5. New onset of facial neuropathy	34
6. Residual new facial neuropathy > grade III[b]	8
7. New onset of trigeminal sensory neuropathy	32
8. Trigeminal motor neuropathy or deafferentation pain syndrome	0
9. Glossopharyngeal neuropathy	1

[a] Clinical follow-up data available for 91 of 92 patients with 92 tumors (99%) with a follow-up mean of 20.5 months (range, 3–36 months).
[b] House-Brackmann facial nerve grading system [21].

does not permit a statistically significant correlation between tumor size and the preservation of hearing or facial nerve function. However, among patients whose treated tumor was smaller than 1 cm in average extrameatal diameter, only one has lost useful hearing and none has had either trigeminal or permanent facial neuropathies after stereotaxic radiosurgery.

Cranial Nerve Imaging

The intracisternal course of the trigeminal nerve from the brainstem to the gasserian ganglia in Meckel's cave is difficult to routinely visualize on CT scans unless it contains enhancing pathology [20]. However, this portion of the trigeminal nerve is routinely discernible on T1-weighted MR imaging even without pathologic enhancement [22, 23]. Previously undetected trigeminal neuropathies developed after radiosurgery in 21 patients. Postoperatively, 12 patients were evaluated with both enhanced and unenhanced MR, three were evaluated solely with contrast-enhanced CT, two with only unenhanced MR, and four with both enhanced CT and enhanced and unenhanced T1-weighted MR.

The cisternal course of the trigeminal nerve was seen clearly in all 18 patients studied with MR but in only one of the seven patients studied with CT (19 total). Pathologic enhancement of the trigeminal nerve was identified in three of these 19 patients (16%) (two had MR and one had CT) (Figs. 8 and 11). In all three patients the clinical onset of trigeminal neuropathy preceded the neuroimaging findings by 2– 9 months (mean, 5.7 months). The cranial nerve enhancement resolved completely over 6 and 11 months, respectively, in two patients (Fig. 11) and was reduced but still present at follow-up after 6 months in the third. A fourth patient with a preexisting trigeminal neuropathy developed subjective worsening of symptoms 4 months after radiosurgery. The trigeminal nerve did not enhance on the 3-month postoperative study but subtle enhancement was present on the 9-month postoperative study that went on to resolve completely by the 20-month postoperative study. Clinical improvement tended to correlate with reduced enhancement in these four patients.

Present imaging techniques did not permit us to assess neuroimaging changes in the facial nerve after radiosurgery for acoustic tumors. The one patient who developed a glossopharyngeal neuropathy after radiosurgery did not have any visible enhancement of the glossopharyngeal nerve on follow-up enhanced MR images.

Discussion

For some patients with acoustic tumors gamma knife stereotaxic radiosurgery is an alternative to surgical removal of the tumor. In a single treatment session, this technique administers a dose of radiation presumably sufficient to cause irreparable cell damage and delayed vascular obliteration [4, 5]. The dose can be delivered to a precisely defined volume of tissue with minimal radiation exposure to the surrounding normal structures. Radiosurgery is notably different from conventional fractionated radiation therapy, which depends on the difference in radiosensitivity between normal and abnormal tissue for its effect and which predominantly affects dividing cells [12, 24]. Although scattered reports suggest that some acoustic tumors may be radiosensitive [25], conventional radiation therapy usually is not effective for histologically benign tumors with generally slow growth rates.

Tumor Size

Interpreting growth rates or detecting delayed tumor shrinkage requires accurate measurement techniques. Our measurement of tumor size was affected most by the difficulty in measuring the tumor height (measurement C). The ±3 mm error resulted from the minimum table increment in the baseline axial CT images. MR can image directly in the coronal and sagittal planes without reconstructions, but, unfortunately, not all patients were able to have either baseline or follow-up MR scans. If preradiosurgical MR images had been available for all patients, the technical measurement error could have been reduced to ±0.5 mm. Our calculations of tumor volumes were performed retrospectively, using calipers on images obtained with a variety of CT or MR techniques. One-dimensional measurement error was magnified further by the third-order equation for calculating volume.

Tumor volumes can be measured directly on a CT console by tracing the tumor margin on each axial slice, calculating the area of the region of interest for each slice, and totaling these areas while adjusting for slice thickness [26, 27]. This method decreases measured tumor-volume error to about

±10% but still is imprecise with small tumors. Thin slices, high-resolution technology, and sufficient IV contrast agent are necessary to optimize tumor visualization. Because many of our follow-up studies were performed at other institutions, for purposes of this study we resorted to a method to measure tumor dimensions using CT and MR hard-copy images. In the future, a uniform protocol for postoperative imaging technique may enable us to gain more accurate measurements, regardless of the institution performing the study.

Norén and associates [5] evaluated patients with acoustic tumors an average of 4 years after stereotaxic radiosurgery. Their *subjective* assessment of tumor size found a decrease in 44% of patients, no change in 42%, and a gradual increase in 14%. Our results show less variation of change in tumor size. We do not know whether this apparent difference in results arises from adoption of a stricter definition of change in tumor size or simply reflects a shorter follow-up interval (mean follow-up of 14.6 months vs 4 years). We previously reported a *subjective* decrease in tumor size in 55% of 40 patients with more than 1 year of neuroimaging follow-up [13], but the present study, using stricter criteria, suggests a 36% tumor shrinkage rate for patients with at least 1 year of neuroimaging follow-up (Table 3). To and colleagues [28] recently reported their analysis of eight patients with acoustic tumors treated by a gamma unit in Sweden. In this study, the investigators calculated tumor-doubling time based on two or more MR scans at least 1 year apart. They noted slow tumor growth in two patients, growth arrest in five patients, and tumor shrinkage in one patient.

Columbo [10] reported neuroimaging results after linear accelerator radiosurgery in eight patients with acoustic tumors who had a mean follow-up time of 18.6 months. Tumor size was described as increased in two patients, unchanged in two, and decreased in three, but no objective assessment of the degree of change in tumor size was given. Hitchcock and coworkers [11] described a single acoustic tumor treated with linear accelerator radiosurgery and presented a 7-month follow-up CT image showing loss of tumor contrast enhancement and "tumor shrinkage." Using a linear accelerator modified for radiosurgery, Friedman [9] treated seven patients with acoustic tumors, but detailed analysis of his results is not yet available. As further experience is gained with this new technique for performing radiosurgery, comprehensive analysis of posttreatment imaging studies will help define its safety and efficacy.

The radiobiological mechanism by which stereotaxic radiosurgery inhibits further tumor growth is not yet well defined. In vitro studies suggest that Schwann cells are irreversibly damaged after single-fraction radiation doses as low as 30 Gy [29, 30]. Postmortem histopathologic studies of treated patients are few. Norén and colleagues [4] examined one patient who died of pneumonia 6 months after radiosurgery. In this case, the tumor had a sharp margin between necrotic and unaffected tumor tissue at the isodose corresponding to 50 Gy. We studied the postmortem histopathologic findings in another patient treated in Sweden, who died of unrelated causes 11 weeks after radiosurgery. The tumor contained an increased amount of proteinaceous material, residual and apparently viable cells, but no necrosis [31]. These limited studies suggest that the tumor-cell response is both time- and dose-dependent [30]. The critical minimal and maximally effective radiosurgical doses have not been precisely determined. Although Norén's group believed doses of 20 Gy at the margin of the tumor were required for tumor control [4, 5], we have found that lower doses still achieve tumor control rates in more than 90% of patients [13, 14].

In microsurgical treatment of tumors, cure is defined as complete tumor resection without evidence of delayed recurrence on follow-up neuroimaging studies. Stereotaxic radiosurgery does not remove the tumor but appears to arrest tumor growth in the majority of patients. After radiosurgery, either absence of tumor growth or tumor shrinkage is considered a satisfactory result. Radiation-induced cell death, tissue necrosis, and replacement of tumor cells with fibroblasts and scarring can lead to either outcome, depending on the histologic composition and cellular density of any given tumor.

To compare the tumor control achieved after radiosurgery with the natural history of untreated acoustic tumors, we reviewed all published reports of untreated acoustic tumor growth rates documented by neuroimaging. To limit anecdotal bias, we only included reported series with at least three patients. After accounting for apparent duplicate publications [32, 33], we were able to find 10 reports describing 199 patients [33–42]. The average age of the patients in this composite natural history series was 59 years (range, 11–81 years) and the average length of neuroimaging follow-up was 2.6 years (range, 0.25–16 years). Tumor growth in these reports was assessed in four different ways: a change in one-dimensional tumor diameter [33, 36, 37, 39, 40], a change in the average two-dimensional tumor diameter [35, 41, 42], a change in one-dimensional tumor diameter as a percentage of the original tumor diameter [38], or as a volumetric tumor doubling time [34]. For the purpose of fair comparison with tumor size changes in our series of patients treated with radiosurgery (which required a 2.6-mm change in average tumor diameter over an average follow-up of 1.7 years), we defined tumor growth in the natural history (control) group as one of the following: an increase in tumor diameter of at least 2 mm/year, a greater than 20% increase from the original tumor diameter, or a volumetric tumor doubling time of 1.5 years or less. On the basis of these criteria, tumor size in the control group increased in 76 cases (38%), was unchanged in 118 (59%), and decreased in five (3%) over an average follow-up period of 2.6 years (Table 6).

Stereotaxic radiosurgery clearly offers improved tumor control in comparison to these untreated historical controls ($p < .001$, chi-square with 2 *df*). To make the argument more forcefully, assume that radiosurgery is an effective treatment for only a subgroup of patients (those 20 patients who had tumor shrinkage) and that the remaining 69 patients were unaffected by the treatment. Tumors in these 69 patients would be expected to have the same growth rates as the untreated tumors. If the natural history data from Table 6 is applied to this group, 26.2 of these tumors should have enlarged, 40.7 should have remained unchanged, and 2.1 should have shrunk. The fact that only four enlarged and 65 remained unchanged strongly suggests that these 65 are

TABLE 6: Comparison of Tumor Control Achieved by Stereotaxic Radiosurgery vs the Untreated Natural History of Acoustic Tumors Based on Historical Controls[a]

	Natural History (Historical Controls) $n = 199$	Stereotaxic Radiosurgery (Univ. of Pittsburgh) $n = 89$
Mean age (range, yrs)	59 (11–81)	60 (14–83)
Mean follow-up (range, yrs)	2.6 (0.24–16)	1–7 (0.25–3)
No. (%) of tumors increased in size	76 (38)	4 (4)
No. (%) of tumors unchanged in size	118 (59)	65 (73)
No. (%) of tumors decreased in size	5 (3)	20 (22)

[a] Outcomes are significantly different $p < .001$, chi-square with 2 degrees of freedom.

examples of tumor control as a result of radiosurgery rather than the natural history of these tumors ($p < 1 \times 10^{-7}$, chi-square with 2 *df*).

The observed variability in the response of tumor size to radiosurgery is unlikely to be the result of incorrect diagnosis in the 66 patients (67 tumors) who did not have a tissue diagnosis. The neuroimaging diagnosis of acoustic tumors has become extremely specific. Of over 150 tumors operated on at our institution over the last 4 years with the characteristic appearance of an acoustic tumor on CT or MR imaging, only one (<1%) has turned out to be anything other than an acoustic tumor by histopathology [43].

Tumor Enhancement

After radiosurgery with the gamma unit, postoperative imaging studies often reveal a loss of intratumoral contrast enhancement. This effect has been postulated to result from radiation-induced vascular injury and occlusion [4]. Obliteration of blood supply to the tumor may be one of the most significant mechanisms controlling tumor growth after radiosurgery. It is not known whether return of intratumoral contrast enhancement represents replacement of avascular necrotic tumor with vascularized scar tissue or the recovery of tumor vascularity.

Complications Detected by Neuroimaging

The presence of communicating hydrocephalus, even in patients with untreated acoustic tumors, is well described, but its rate of occurrence is poorly documented. In patients with acoustic tumors, hydrocephalus may result from elevated CSF protein levels [4]. Stereotaxic radiosurgery could lead to further rises in CSF protein as a result of tumor necrosis and thus could contribute to the development of hydrocephalus by overwhelming the brain's CSF resorptive capacity [4, 5]. While CSF protein concentrations were elevated in three patients who developed hydrocephalus after radiosurgery, the degree of elevation was modest.

The cause of signal changes in areas of the brain near the tumor remains controversial. The most likely causes include edema and/or blood-brain barrier breakdown in the adjacent parenchyma. These imaging changes are characterized by absence of hypointensity on T1-weighted scans, their temporary nature, and few associated neurologic symptoms despite their appearance in critical areas of the adjacent pons and cerebellar peduncle. We did observe neurologic symptoms (contralateral hemiparesis) in a patient with a petrous apex meningioma in whom increased T2 signal developed within the brainstem [44]. The patient's tumor was treated with the gamma knife using three isocenters delivering 20 Gy to the tumor margin at the 50% isodose line. Both the hemiparesis and the MR changes resolved within 7 months. Possible primary causes for the development of edema or blood-brain barrier breakdown include demyelination or vasculopathy, which have been reported to occur with delayed onset after conventional radiotherapy [45–47]. Although these signal changes probably represent delayed radiation effects, they are not likely to be radiation necrosis, since they appear to have resolved over time in at least two patients.

The cause of the trigeminal nerve enhancement seen in four patients with sensory trigeminal neuropathy is most likely related to blood-brain barrier breakdown. Once again, whether this blood-brain barrier breakdown is related to demyelination, vasculopathy, or both remains unresolved. The fact that the rate of trigeminal neuropathy significantly correlated with an average tumor diameter greater than 1 cm suggests that the proximity of the nerve to the irradiated tumor volume is an important factor and could support either possibility. The fact that the rate of trigeminal neuropathy significantly correlated with a loss of intratumoral contrast enhancement suggests that vasculopathy may play a significant role in the pathophysiology of the trigeminal dysfunction.

Stereotaxic radiosurgery is an important alternative treatment for selected patients with acoustic tumors. There is no mortality or major perioperative morbidity, hospitalization time and costs are reduced compared with microsurgery, and hearing preservation and facial neuropathy rates are comparable to those of the best published microsurgical series. Although the trigeminal neuropathy rate may be greater after radiosurgery compared with modern microsurgical series, these trigeminal neuropathies are usually mild, transient, and nondebilitating.

Modern, high-resolution neuroimaging is necessary for adequately assessing the response of acoustic tumors to stereotaxic radiosurgery. MR before and after radiosurgery is the most sensitive imaging tool to evaluate tumor response, the presence or absence of adjacent parenchymal signal changes, and ventricular size. Narrow slices and multiplanar imaging using unenhanced, prolonged TR and enhanced, short TR sequences are imperative. Accurate tumor dimensions can be measured directly on the computer console, obviating cumbersome and less accurate retrospective analysis using calipers. If MR studies cannot be obtained, CT is the next best imaging alternative. When CT is used, thin slices, sufficient IV contrast agent, and multiplanar reformatting are valuable for adequately monitoring the effects of radiosurgery.

Neuroimaging is an important quality control tool for radiosurgery and is a necessary supplement to observations regarding clinical response. Our analysis, using strict measurement criteria, suggests a high initial tumor control rate of 96%

TABLE 7: Postoperative Neuroimaging Changes[a]

Neuroimaging Change	No. (%) of Patients
1. Tumor shrinkage	20 (22)
2. Tumor stasis	65 (73)
3. Tumor growth	4 (4)
4. Loss of intratumoral contrast enhancement[b]	66 (79)
5. Communicating hydrocephalus	4 (4)
6. New increased T2 signal in adjacent brain	8 (9)
7. New onset of cranial nerve enhancement	4 (4)

[a] Neuroimaging follow-up available in 88 of 92 patients with 89 tumors (97%) with a follow-up mean of 14.6 months (range, SD 8.8 months).

[b] Follow-up imaging including contrast-enhanced studies in 83 of 88 patients with neuroimaging follow-up (94%).

with a mean follow-up of 14.6 months, and a 22% rate of significant tumor shrinkage (Table 7). The rate of tumor shrinkage appears to be time-dependent and increases to 36% of patients followed with neuroimaging for a minimum of 1 year. Further studies of the rate of long-term tumor control and the frequency of treatment complications are needed.

ACKNOWLEDGMENTS

We thank Robert J. Coffey for allowing us to include 15 of his patients in this study, David Bissonette for assisting with management of the computer data base, Helene Marion for editorial assistance, and Mary Ann Vincenzini and Charlene Thompson for preparation of the manuscript.

REFERENCES

1. Lunsford LD, Flickinger J, Lindner G, Maitz A. Stereotactic radiosurgery of the brain using the first United States 201 cobalt-60 source gamma knife. *Neurosurgery* **1989**;24:151–159
2. Lunsford LD, Flickinger JC, Coffey RJ. Stereotactic gamma knife radiosurgery: initial North America experience in 207 patients. *Arch Neurol* **1990**;47:169–175
3. Lunsford LD, Maitz A, Lindner G. First United States 201 source cobalt-60 gamma knife unit for radiosurgery. *Appl Neurophysiol* **1987**;50: 253–256
4. Norén G, Arndt J, Hindmarsh T. Stereotactic radiosurgery in cases of acoustic neurinoma: further experience. *Neurosurgery* **1983**;13:12–22
5. Norén G, Arndt J, Hindmarsh T, Hirsch A. Stereotactic radiosurgical treatment of acoustic neurinomas. In: Lunsford LD, ed. *Modern stereotactic neurosurgery*. Boston: Martinus Nijhoff, **1988**:481–489
6. Hirsch A, Norén G. Audiological findings after stereotactic radiosurgery in acoustic neurinomas. *Acta Otolaryngol (Stockh)* **1988**;106:244–256
7. Walton L, Bomfort CK, Ransden D. The Sheffield stereotactic radiosurgery unit: physical characteristics and principles of operation. *Br J Radiol* **1987**;60:897–906
8. Friedman WA, Bova FJ. The University of Florida radiosurgery system. *Surg Neurol* **1989**;32:334–342
9. Friedman WA. Linac radiosurgery. *Neurosurg Clin North Am* **1990**;1:991–1008
10. Columbo F. Linear accelerator radiosurgery: a clinical experience. *J Neurosurg Sci* **1989**;33:123–125
11. Hitchcock E, Kitchen G, Dalton E, Pope B. Stereotactic Linac radiosurgery. *Br J Neurosurg* **1989**;3:305–312
12. Leksell L. A note on the treatment of acoustic tumors. *Acta Chir Scand* **1971**;137:763–765
13. Flickinger JC, Lunsford LD, Coffey RJ, et al. Radiosurgery of acoustic neurinomas. *Cancer* **1991**;67:345–353
14. Linskey ME, Lunsford LD, Flickinger JC. Radiosurgery for acoustic neurinomas: early experience. *Neurosurgery* **1990**;26:736–745
15. Wayman JW, Dutcher PO, Manzione JV, et al. Gadolinium-DTPA-enhanced magnetic resonance scanning in cerebellopontine angle tumors. *Laryngoscope* **1989**;99:1167–1170
16. Wilms G, Decrop E, Plets C, et al. Magnetic resonance imaging in acoustic neurinoma. Comparison with CT. *J Belge Radiol* **1989**;72:151–158
17. Flickinger JC. An integrated logistic formula for prediction of complications from radiosurgery. *Int J Radiat Oncol Biol Phys* **1989**;17:879–885
18. Flickinger JC, Lunsford LD, Wu A, Maitz AH, Kalend AM. Treatment planning for gamma knife radiosurgery with multiple isocenters. *Int J Radiat Oncol Biol Phys* **1990**;18:1495–1501
19. Flickinger JC, Maitz A, Kalend A, Lunsford LD, Wu A. Treatment volume shaping with selective beam blocking using the Leksell gamma unit. *Int J Radiat Oncol Biol Phys* **1990**;19:783–789
20. Gardner G, Robertson JH. Hearing preservation in unilateral acoustic neuroma surgery. *Ann Otol Rhinol Laryngol* **1988**;97:55–66
21. House JW, Brackmann DE. Facial nerve grading system. *Otolaryngol Head Neck Surg* **1985**;93:146–147
22. Vitte E, Bensimow JL, Baulac M. Radiological studies in trigeminal nerve pathology. *Arch Otorhinolaryngol* **1989**;246:262–264
23. Daniels DL, Pech P, Pojunas KE, et al. Trigeminal nerve: anatomic correlation with MR imaging. *Radiology* **1986**;159:577–583
24. Leksell DG. Special stereotactic techniques: stereotactic radiosurgery. In: Heilbrun MP, ed. *Stereotactic neurosurgery*. Baltimore: Williams & Wilkins, **1988**:195–209
25. Wallner KE, Sheline GE, Pitts LH, Wara WM, Davis RL, Bordray FB. Efficacy of irradiation for incompletely excised acoustic neurilemmomas. *J Neurosurg* **1987**;67:858–863
26. Firsching RP, Doz P, Fischer A, Peters R, Thun F, Klug N. Growth rate of incidental meningiomas. *J Neurosurg* **1990**;77:545–547
27. Lunsford LD, Levine G, Gumerman LW. Comparison of computerized tomographic and radionuclide methods in determining intracranial cystic tumor volumes. *J Neurosurg* **1985**;63:740–744
28. To SY, Lufkin RB, Rand R, Robinson JD, Hanafee W. Volume growth rate of acoustic neuromas on MRI post-stereotactic radiosurgery. *Comput Med Imaging Graph* **1990**;14:53–59
29. Anniko M. Early morphological changes following gamma irradiation. *Acta Pathol Microbiol Immunol Scand [A]* **1981**;89:113–124
30. Anniko M, Arnor J, Norén G. The human acoustic neurinoma in organ culture II. Tissue changes after gamma irradiation. *Acta Otolaryngol (Stockh)* **1981**;91:223–235
31. Thompson BG, Coffey RJ, Flickinger JC, Lunsford LD. Stereotactic radiosurgery of small intracranial tumors: neuropathological correlation in three patients. *Surg Neurol* **1990**;33:96–104
32. Clark WC, Moretz WH, Acker JD, et al. Nonsurgical management of small and intracanalicular acoustic tumors. *Neurosurgery* **1985**;16:801–803
33. Gardner G, Moretz WH, Robertson JH, et al. Nonsurgical management of small and intracanalicular acoustic tumors. *Otolaryngol Head Neck Surg* **1986**;94:328–333
34. Laasonen EM, Troupp H. Volume growth rate of acoustic neurinomas. *Neuroradiology* **1986**;28:203–207
35. Nedzelski JM, Canter RJ, Rowed DW, et al. Is no treatment good in the management of acoustic neuromas in the elderly? *Laryngoscope* **1986**;96:825–829
36. Silverstein H, McDaniel A, Norrell H, et al. Conservative management of acoustic neuroma in the elderly patient. *Laryngoscope* **1985**;95:766–770
37. Thomsen J, Tos M. Acoustic neuroma: Clinical aspects, audiovestibular assessment, diagnostic delay and growth rate. *Am J Otol* **1990**;11:12–19
38. Valbsddoti GE, Guzman M. Growth rate of acoustic neuromas. *Am J Otol* **1989**;10:174–176
39. Wazen J, Silverstein H, Norrell H, et al. Preoperative and postoperative growth rates in acoustic neuromas documented with CT scanning. *Otolaryngol Head Neck Surg* **1985**;93:151–155
40. Wiet RJ, Young NM, Monsell EM, et al. Age considerations in acoustic neuroma surgery: the horns of a dilemma. *Am J Otol* **1989**;10:177–180
41. Bederson JB, Von Ammon K, Wichmann WW, Yasargil MG. Conservative treatment of patients with acoustic tumors. *Neurosurgery* **1991**;28: 646–651
42. Zollner C, Bockenheimer S. The growth rate of acoustic neuromas: a report of three cases. *Arch Otorhinolaryngol* **1985**;241:259–264
43. Linskey ME, Jannetta PJ, Martinez AJ. A vascular malformation mimicking an intracanalicular acoustic neurilemoma. Case Report. *J Neurosurg* **1991**;74:516–519
44. Kondziolka D, Lunsford LD, Coffey RJ, Flickinger JC. Stereotactic radiosurgery of meningiomas. *J Neurosurg* **1991**;74:552–559
45. Lampert PW, Davis RL. Delayed effects of radiation on the human central nervous system: "early" and "late" delayed reactions. *Neurology* **1964**;14:912–917
46. Liebel SA, Sheline GE. Radiation therapy for neoplasms of the brain. *J Neurosurg* **1987**;65:1–22
47. Sheline GE, Wara WM, Smith V. Therapeutic irradiation and brain injury. *Int J Radiat Oncol Biol Phys* **1980**;6:1215–1228